Biochemistry (Moscow), Vol. 68, No. 3, 2003, pp. 275-285. Translated from Biokhimiya, Vol. 68, No. 3, 2003, pp. 336-348.
Original Russian Text Copyright © 2003 by Tonevitsky, Agapov, Moisenovich, Maluchenko, Pashkov, Balashova, Kirpichnikov.

ACCELERATED PUBLICATION

A New Antigenic Epitope Appears in the Catalytic Subunit of Viscumin during Intracellular Transport

A. G. Tonevitsky[1]*, I. I. Agapov[1], M. M. Moisenovich[1], N. V. Maluchenko[1], V. S. Pashkov[2], T. A. Balashova[2], and M. P. Kirpichnikov[1]

[1]School of Biology, Lomonosov Moscow State University, Moscow, 119899 Russia; fax: (095) 196-0522; E-mail: tonevits@genetika.ru
[2]Shemyakin and Ovchinnikov Institute of Bioorganic Chemistry, Russian Academy of Sciences, ul. Miklukho-Maklaya 16/10, Moscow, 117997 Russia; fax: (095) 335-2733; E-mail: aars@siobc.ras.ru

Received November 10, 2002
Revision received December 17, 2002

Abstract—The plant toxin viscumin (60 kD) consists of B- ("binding") and A- ("active") subunits joined by a disulfide bond. The B-subunit is a lectin interacting with galactose-containing glycolipids and glycoproteins of the cell surface. The A-subunit possesses N-glycosidase activity which modifies 28S ribosomal RNA. This results in irreversible inhibition of protein synthesis. After binding and receptor-mediated endocytosis viscumin-containing vesicles are transported to endoplasmic reticulum where the A- (catalytic) subunit is subsequently translocated to cytosol. It is possible that translocation of A-subunit requires its unfolding. For identification of epitopes which might appear during such unfolding, we developed hybridomas producing monoclonal antibodies against denatured viscumin A-chain. Resistance of hybridoma cells to cytotoxic action of viscumin suggests antibody–toxin interaction inside these cells. TA7 hybridoma cells against an epitope which appears only in denatured viscumin are insensitive to the toxin. This suggests that antibody–toxin interaction occurs before transmembrane translocation of the catalytic A-chain into the cytoplasm. Consequently, toxin resistance of TA7 hybridoma cells implies the appearance of a new epitope in viscumin during its intracellular transportation inside of vesicles. Sixty five octapeptides have been synthesized and epitopes have been identified for monoclonal TA7 antibody and immune mouse serum by means of ELISA. Based on the epitopic mapping the peptide A96-ETHLFTGT-T105 was chemically synthesized and binding of this peptide to the monoclonal antibody TA7 and conformation of antigenic determinant (L100-FTGT-T105) was investigated by means of ^{1}H-NMR spectroscopy.

Key words: viscumin, ricin, monoclonal antibodies, epitopic analysis, ^{1}H-NMR spectroscopy

Viscumin (mistletoe lectin I, MLI) is a member of type II ribosome inactivating proteins (RIPs), which also include such plant proteins as ricin, abrin, and modecin. These proteins are highly cytotoxic for mammalian cells [1]. Even one toxin molecule penetrated into the cytosol of the host cell can cause its death, and so RIPs are considered as promising agents for the development of addressed delivery of cytostatics [2]. The process of MLI penetration into cells begins with interaction of its B-subunit with cell surface galactose-containing receptors followed by toxin internalization inside cells via receptor-mediated endocytosis. The toxin inside vesicles passes through endosomal compartments, the Golgi apparatus, to endoplasmic reticulum. After reduction of the disulfide bond between A- and B-subunits the catalytic A-subunit of viscumin (MLA) enters the cytosol and this represents the final stage of toxin transport [3]. Owing to the ability for transmembrane transportation toxins are employed as vectors for delivery of various peptides into cytosol and this is used for the development of a new generation of vaccines [4]. The mechanism responsible for transmembrane transport of toxins remains unclear. According to one hypothesis toxins employ a retrotranslocation system for transition from endoplasmic reticulum into cytosol [5]. The retrotranslocation system operating in all normal cells exports incorrectly folded proteins from endoplasmic reticulum cisterns. It is possible that in these cisterns toxins may undergo conformational changes (e.g., partial unfolding) and thus mimic incorrectly folded proteins. Previously it was shown that viscumin dissociates into binding (B) and catalytic (A) subunits before the onset of translocation [6] and this may cause exposure of addi-

Abbreviations: MLA) A-subunit of viscumin; MLI) viscumin (mistletoe lectin I).

* To whom correspondence should be addressed.

0006-2979/03/6803-0275$25.00 ©2003 MAIK "Nauka/Interperiodica"

tional hydrophobic regions. Incorrectly folded proteins exported to cytosol by the retrotranslocation system are labeled with ubiquitin for subsequent proteasome degradation [7]. In contrast to ricin and abrin, MLA lacks lysine residues (representing potential sites for ubiquitinylation) and so viscumin may employ this system for transport into the cytosol without potential "danger" of proteasome degradation. Previously it was shown that MLA causes liposome aggregation in model systems [8] and so it is possible that translocation of MLA does not involve special protein carriers and it does occur via direct interaction with membranes of intracellular compartments. In the present study we have searched for new epitopes in MLA during intracellular transport of MLI. For this purpose we have developed a model employing hybridomas producing antibodies against various epitopes of viscumin [9] (Fig. 1). The resistance of hybridomas to this toxin is determined by antibody–toxin interaction inside compartments; this prevents transmembrane transfer of the toxin into the cytosol [10]. Thus, change in toxin structure inside the cell (i.e., the appearance of new antigenic epitopes) can be detected by attenuation of its cytotoxic activity with respect to the hybridoma cells producing antibodies against this epitope. Analyzing viscumin activity on the panel of hybridomas against denatured MLA we have found hybridoma TA7 resistant to the toxin action. The epitope for the monoclonal antibody TA7 was mapped, chemically synthesized, and it three dimensional structure was determined by ^{1}H-NMR spectroscopy.

MATERIALS AND METHODS

Toxins and their subunits. Viscumin isolated from *Viscum album* was kindly presented by U. Pfluller (Institute of Phytochemistry, Vitten-Herdeke, Vitten, Germany). Ricin from *Ricinus communis* seeds and toxin subunits were isolated as described [11, 12]. Purity of preparations was monitored by electrophoresis and enzyme-linked immune analysis. Protein biotinylation was carried out using N-hydroxysuccinimide ester of biotinamidocaproate (Sigma, USA) according to the supplier's recommendations.

Preparation of hybridomas. Balb/C mice (Stolbovaya animal house, Moscow Region) were immunized with isolated MLA (2.5-5 μg per mouse) with Freund's complete adjuvant. Immune spleen lymphocytes and myeloma sp2/0 cells were fused in polyethylene glycol 4000. Myeloma sp2/0 and hybridoma cells were cultivated using RPMI-1640 medium supplemented with 10% embryonic calf serum at 37°C in a humidified atmosphere of 5% CO_2/95% air. Hybridoma cloning was carried out by the method of limiting dilutions. Monoclonal antibodies were isolated from ascites liquid using affinity chromatography on protein A-Sepharose.

Enzyme linked immunosorbent assay (ELISA). Viscumin (MLI) and its isolated catalytic A-subunit (MLA) were used as antigens. Antibody activity was assayed by the ELISA method using three systems differing by conformational state of the antigen.

1. Adsorbed antigen. The antigen (10 μg/ml) in phosphate buffered saline (PBS), pH 7.5, was adsorbed on the bottom of the immunological 96-well plate for 16 h at 4°C. The plate was washed with the same PBS containing 0.05% Tween-20 and BSA (1 mg/ml) and incubated with biotinylated antibodies (1 μg/ml) at room temperature for 1 h. The plate was washed and incubated with a conjugate (streptavidin–peroxidase) at room temperature for 1 h. After washing and subsequent addition of a substrate mixture absorbance was read at 492 nm using a Multiscan spectrophotometer (LKB, Sweden).

2. Native antigen. Monoclonal antibodies (10 μg/ml) in PBS were adsorbed on the bottom of the 96-well plate for 16 h at 4°C. The plate was washed with the same PBS containing 0.05% Tween-20 and BSA (1 mg/ml) and incubated with biotinylated antigen (1 μg/ml) at room temperature for 1 h. The plate was washed and incubated with the streptavidin–peroxidase conjugate at room temperature for 1 h. After washing and subsequent addition of the substrate mixture, absorbance was read at 492 nm using the Multiscan spectrophotometer.

3. Denatured antigen. Monoclonal antibodies (10 μg/ml) in PBS were adsorbed on the bottom of the 96-well plate for 16 h at 4°C. The plate was washed with the same PBS containing 0.05% Tween-20 and BSA (1 mg/ml) and incubated at room temperature for 1 h with biotinylated antigen (1 μg/ml) pretreated at 100°C for 3 min. The plate was washed and incubated with the streptavidin–peroxidase conjugate at room temperature for 1 h. After washing and subsequent addition of the substrate mixture absorbance was read at 492 nm using the Multiscan spectrophotometer.

For determination of cross-reactivity of monoclonal antibodies we used the competitive ELISA method. The antigen was adsorbed on the plate and the interaction with the first biotinylated monoclonal antibody was inhibited by addition of 100-fold molar excess of the second antibody.

Determination of immunogenic sites and their chemical synthesis. Possible immunogenic sites of viscumin were predicted on the basis of its tertiary structure [13] using software for calculation of exposure of amino acid residues [14] and taking into consideration temperature B-factor values, secondary structure, and variability of amino acid sequences in homologous proteins [15]. Sites containing exposed amino acids (representing more than 70% of the amino residue area), elements of secondary structure (mainly β-turns) and sites flexible by B-factors were considered as the most immunogenic sites of MLA. Based on this analysis, we synthesized 65 octapeptides overlapping by seven residues. These octapeptides cover

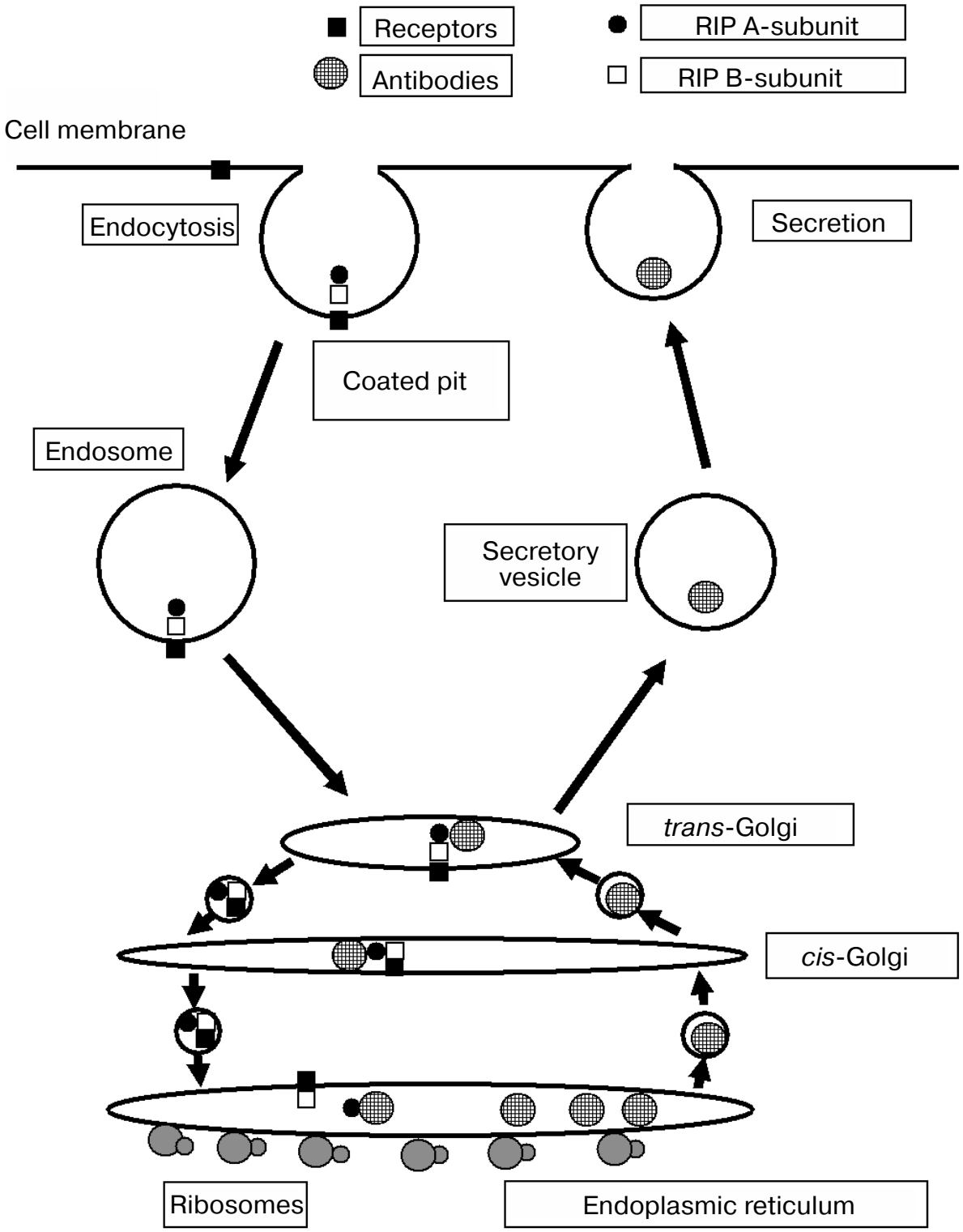

Fig. 1. Scheme of intracellular viscumin transport in the hybridoma cell. The toxin inside endosome reaches Golgi apparatus and appears (in retrograde manner) in the lumen of endoplasmic reticulum. Antibodies produced by the cell are also accumulated within the lumen of endoplasmic reticulum and then they are delivered (inside vesicles in anterograde manner) through Golgi apparatus to the cell surface and secreted. Anterograde and retrograde transportation is achieved by sequential and persistent fusion of membrane vesicles. Toxin and antibody routes may intersect and this is accompanied by toxin–antibody complex formation which inhibits translocation of catalytic A-subunit (MLA) into cytosol.

the following stretches of primary structure of viscumin: 1-13, 31-52, 72-108, 112-127, 196-206, 210-229, and 248-255. Octapeptides bound to polyethylene needles containing di-β-alanine spacer (Chiron Technologies, Australia) were synthesized by the method of activated ethers, using pentafluorophenyl ethers of Nα-Fmoc-L-amino acids (Cambridge Research Biochemicals, England) in the presence of 1-hydroxybenzotriazole (Merck, Germany), as described earlier [16].

Peptide ELISA. Enzyme-linked immune analysis using mouse antiserum against MLA was carried out as described in [16] with some modifications. Serum from viscumin-immunized mice was diluted 1000 times with PBS containing 0.1% Tween-20 and 50% fat-free milk. Peroxidase-labeled antibodies against mouse immunoglobulins (Calbiochem, Switzerland; dilution 1 : 10,000) were used as secondary antibodies. Before each cycle of analysis peptides were washed by ultrasonic treatment (using a Finnsonic ultrasonic washer, Finland) in 0.1 M sodium phosphate buffer, pH 7.2, containing 1% SDS and 0.1% 2-mercaptoethanol at 60°C and then twice with water at the same temperature, and finally with boiling methanol. Enzyme-linked immune analysis of peptides was carried out in similar manner using monoclonal antibodies against viscumin; antibody concentration in samples was 5 μg/ml.

Evaluation of cytotoxic activity of the toxins. Cytotoxic effect was evaluated by cell viability in the presence of toxins. Cell viability was assessed by the MTT test (MTT, 3-[4,5-dimethylthiazol-2-yl]-2,5-diphenyl tetrazolium bromide, Sigma) in a 96-well plate as described [17]. Initial cell concentration was 50,000 per well. Various toxin preparations were compared in terms of LD_{50} (toxin concentration required for death of 50% cells). Staining of cells cultivated without toxins was denoted as 100%. Ricin sharing with viscumin the mechanism of cytotoxic action was used as control for nonspecific resistance of cells to toxins [1]. Myeloma sp2/0 cell line employed for hybridization was used as the control cell line which does not produce antibodies against viscumin.

Peptides. Chemically synthesized peptide corresponding to amino acid stretch of MLA A96-ETHLFTGT-T105-NH_2 was kindly presented by A. Yu. Surov (Shemyakin and Ovchinnikov Institute of Bioorganic Chemistry, Russian Academy of Sciences, Moscow).

^{1}H-NMR spectra (500 and 600 MHz) were recorded in ampoules with external diameter of 5 mm using spectrometers DRX 500 (Bruker, Germany) and UNITY 600 (Varian, USA). Suppression of water signals in ^{1}H-NMR spectra was carried out using sequential impulses WATERGATE [18]. Values for chemical shifts of proton signals were measured versus ^1H_2O signal; at 30°C chemical shift of ^1H_2O signal is 4.75 ppm from sodium 2,2-dimethyl-2-silapentane-5-sulfonate. Signal reference in peptide ^{1}H-NMR spectra was obtained during analysis of spectra by total correlation spectroscopy (TOCSY) (time for mixing of magnetic components was 0.8 sec) and rotating frame Overhauser effect spectroscopy (ROESY) (time for mixing of magnetic components was 0.4 sec). All measurements of 1-3 mM peptide solutions in mixture ^1H_2O–^2H_2O (9 : 1), pH 3.5-5.5, were carried out at 30°C.

Transferred nuclear Overhauser effect from antibody protons was registered as described earlier [19]. Values of the transferred effect were calculated using ratio $(I_{TRNOE}/I_{REF})\cdot 100$, where I_{TRNOE} and I_{REF} are intensities of analogous signals in the differential spectrum of nuclear effect and in the reference spectrum, respectively. (Radiofrequency field γH_2 of 60 Hz was applied to the free region of the spectrum.) For calculation of values of transferred Overhauser effect for peptide signals located in the region of 7-9 ppm differential effect spectra obtained using additional radiofrequency field applied at 0.5 ppm were used. For peptide signals located within 0.8-4.0 ppm the values of transferred nuclear effect were calculated from differential spectra of this effect; these spectra were obtained using additional radiofrequency field applied at 6.7 ppm. Such approach avoids large errors in evaluating the degree of contact between peptide protons with antibody surface, because this approach excludes cases when a proton of the peptide–antibody complex is influenced by an additional radiofrequency field.

Conformations of A96-T105 peptide in the peptide–antibody complex were calculated using DYANA software (Institute of Molecular Biology and Biophysics, Federal High Technical School, Zurich, Switzerland) [20] and limitations for inter-proton distances. Upper limitations for these distances were calculated using the standard DYANA procedure from volumes of cross-peaks measured in NOESY spectrum (nuclear Overhauser effect spectroscopy) (time for mixing of magnetic components was 0.1 sec) of the mixture of peptide and monoclonal TA7 antibody (8 : 1), pH 5.1, at 30°C. In this spectrum the cross-peaks between proton pairs of *i*-th CαH and *i*-th and (*i* + 1)-th NH groups of residues of primary structure were registered. (Maximal distance between these proton pairs can be 2.8 and 3.6 Å.) At the same time several cross-peaks between protons of NH and CβH of the same amino acid residue where maximal distance may reach 4.1 Å were absent. Taking into consideration all these data we introduced lower limitations for the inter-proton distances. According to these limitations lack of a cross-peak between protons was considered as evidence that the distance between corresponding protons exceeded 3.6 Å. We selected 20 of 100 conformers randomly generated and optimized using DYANA; these conformers satisfied experimental limitations for inter-proton distances.

For determination of relative susceptibility of hydrogen atoms of the fragment H99-T105 to contacts with

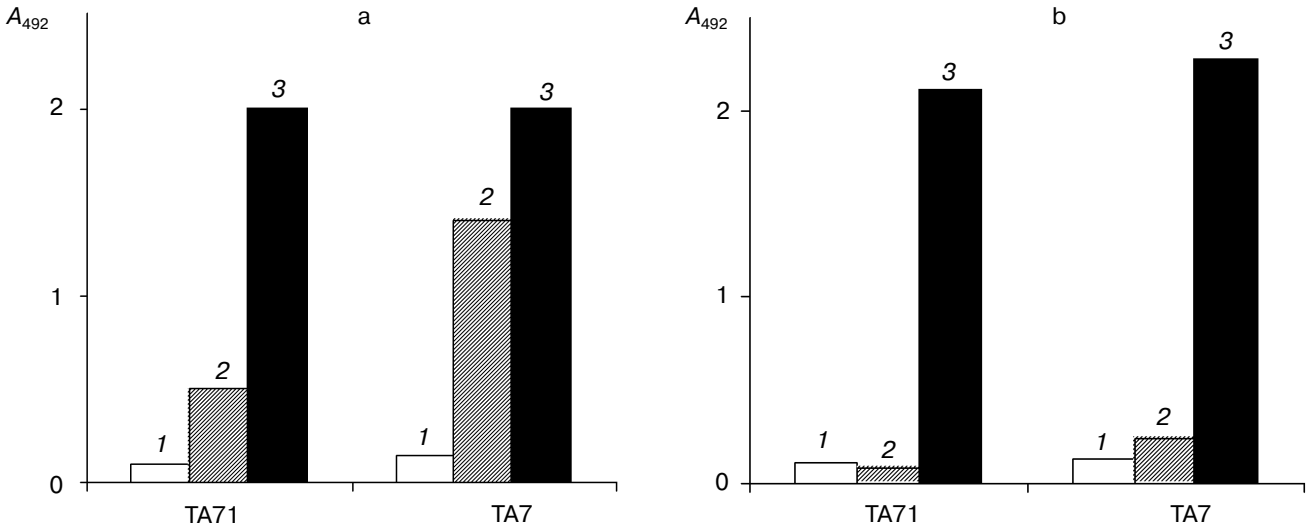

Fig. 2. Interaction of monoclonal antibodies TA7 and TA71 with native (*1*), denatured (*2*) and adsorbed on the immunological plate (*3*) MLA (a) or MLI (b).

solvent (radius of 1.4 Å) we used MOLMOL software (Institute of Molecular Biology and Biophysics, Federal High Technical School, Zurich) [21]. This software was also employed for identification of secondary structure of the fragment H99-T105 from either the X-ray model of MLA or within the complex peptide–monoclonal antibody TA7 (and also for design of Fig. 8, see below).

RESULTS

Preparation and analysis of specificity of monoclonal antibodies. Immunization of mice with MLA was carried out in the presence of Freund's complete adjuvant, which may influence protein conformation by increasing exposure of internal hydrophobic fragments [22]. For hybridoma preparation by fusing with myeloma sp2/0 we used splenocytes from the immune mouse the serum of which reacted with denatured MLA at dilution 1 : 500,000.

Monoclonal antibodies were screened by ELISA using viscumin or its catalytic subunit adsorbed on the immunological plate or subjected to heat denaturation (Fig. 2). Seven antibodies interacting with denatured viscumin were recognized. The use of competitive ELISA allowed these antibodies to be separated into two groups characterized by different specificity. Six antibodies formed one group whereas only one antibody (TA7) represented the second group. In subsequent comparative experiments we used one antibody from each group (TA71 and TA7; Fig. 3). Both antibodies reacted with MLA and MLI adsorbed on the plate and with the denatured antigens. Neither antibody reacted with the native peptides. Thus, adsorption of toxin or its catalytic subunit on the immunological plate was accompanied by denaturation or partial unfolding of these proteins and this resulted in appearance of new epitopes. It is possible that the toxin may undergo such (or similar) changes inside cells, for example, during the interaction of MLA with hydrophobic membrane.

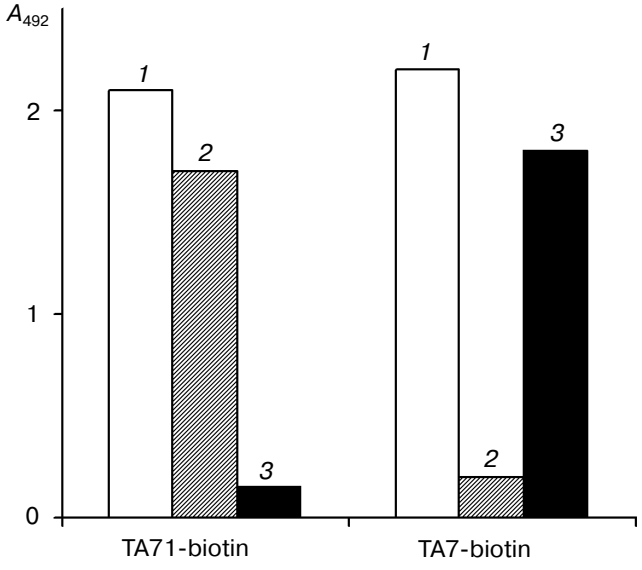

Fig. 3. Competitive inhibition of interaction of biotinylated monoclonal antibodies with adsorbed viscumin by 100-fold molar excess of antibodies. Viscumin was adsorbed on the immunologic plate and biotinylated antibodies TA71 and TA7 (*1*) were added in the presence of the molar excess of TA7 (*2*) or TA71 (*3*). The reaction was read after the addition of streptavidin–peroxidase conjugate.

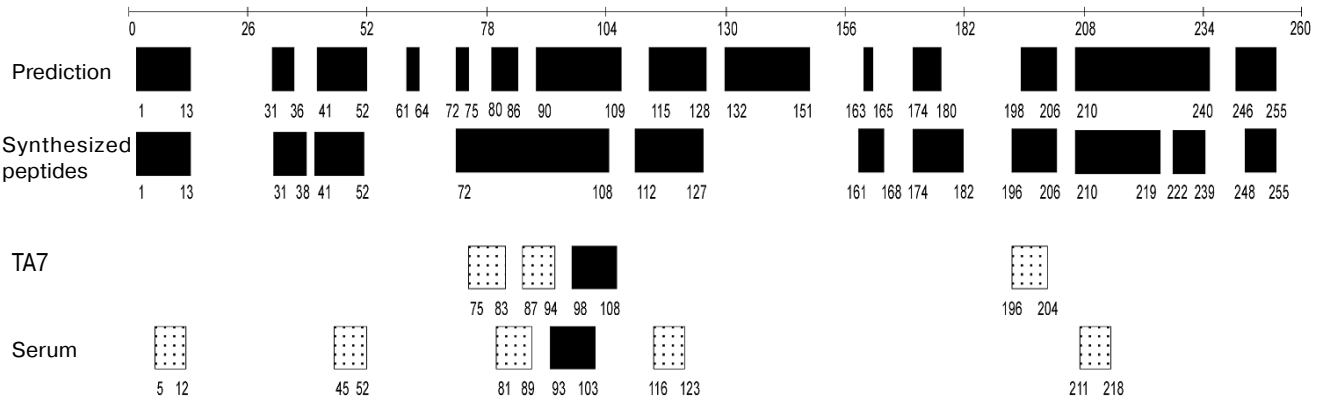

Fig. 4. Scheme of epitope mapping of MLA. Epitope analysis of monoclonal antibodies was carried out by means of ELISA (see "Materials and Methods" section). Absorbance data: 0.5-3 (dark rectangles), 0.05-0.5 (light rectangles).

Epitope mapping. Based on algorithms of prediction we selected the most probable immunogenic regions of MLA (31% of the whole sequence) and synthesized corresponding octapeptides (Fig. 4, top). Peptides 1-6 covered the region of amino acid sequence including residues 1-13; peptide 7 covered residues 31-38; peptides 8-12 – residues 41-52; peptides 13-42 – residues 72-108; peptides 43-51 – residues 112-127; peptide 52 – residues 161-168; peptides 53-54 – residues 174-182; peptides 55-58 – residues 196-206; peptides 59-61 – residues 210-219; peptide 62 – residues 222-229; peptides 63-64 – residues 231-239; peptide 65 – residues 248-255. The interaction of TA7 antibody with peptides was studied by the ELISA method. Serum from the mouse used as a splenocyte donor for hybridization served as positive control. Antibodies of the immune serum bound to the following sites of viscumin primary structure, including residues 5-12, 45-52, 81-90, 93-103, 116-123, and 211-218 (Fig. 4). Peptides corresponding to amino acid residues 93-103 exhibited the most effective interaction with antibodies. Monoclonal antibody TA71 as well as other antibodies of the first group reacted mainly with peptides representing residues 93-103 (epitope AETHL). Antibody TA7 effectively interacted with peptides representing residues 98-108 (epitope FTGTT) (Fig. 4). Data of X-ray analysis of the viscumin molecule [13] indicate that the fragment 93-103 of MLA is a loop, this highly immunological site being overlapped with the TA7 epitope. The comparison of antigenic properties of two epitopes (AETHL and FTGTT) by the method of Hopp and Woods [23] revealed more pronounced antigenic properties of the AETHL site. This probably accounts for larger number of monoclonal antibodies in the first group which we found in the process of screening.

Hybridoma resistance. Table 1 shows cytotoxic activity (LD_{50}) of viscumin with respect to hybridoma cells. Using control cell line sp2/0 as a reference all hybridomas may be subdivided into two groups by their resistance to cytotoxic effect of viscumin: resistant hybridomas (TA7) and all other hybridomas (TA71-TA77). The resistance of hybridomas forming the latter group is comparable to that of control cell line sp2/0. Nonspecific resistance of hybridomas to toxin effect was tested with ricin. TA7-hybridoma which was 15 times more resistant to viscumin than the control cell line sp2/0 was characterized by the same resistance to ricin as sp2/0 cells. Previously we demonstrated that resistance of hybridomas is determined by specificity rather than affinity of the producing antibodies [9]. It is possible that viscumin site(s) recognized by TA7-antibodies is a "key" site for manifestation of cytotoxicity and so we have investigated the structure of this antigenic determinant of TA7 antibody in more detail.

Structure of TA7 antigenic epitope in its complex with monoclonal antibody. Involvement of groups essential for binding of peptide A96-ETHLFTGT-T105-NH_2 to TA7 antibody was investigated using the transferred nuclear Overhauser effect, which appears on signals of a free peptide during irradiation of antibody protons of

Table 1. Cytotoxic effects of viscumin and ricin (LD_{50}) on hybridoma cells producing antibodies against A-subunit of viscumin

Toxin	Hybridoma		
	TA7	TA71	sp2/0
Viscumin	$3 \cdot 10^{-11}$ M	$1.5 \cdot 10^{-12}$ M	$2 \cdot 10^{-12}$ M
Ricin	$3 \cdot 10^{-13}$ M	$2.5 \cdot 10^{-13}$ M	$3 \cdot 10^{-13}$ M

peptide–antibody complex with an additional radiofrequency field. Figures 5 and 6 show comparative spectra (a) and differential spectra of transferred nuclear Overhauser effect (b). The values of signals are directly dependent on contact of the corresponding peptide group with surface protons of the antibody.

Values of transferred nuclear effect increased almost linearly with the increase of duration of additional radiofrequency field application (τ_{ir}, Table 2). This suggests the absence of spin diffusion effects and therefore it allows to use values of transferred nuclear effect measured at relatively high values of τ_{ir} (0.6 sec). Maximal values of transferred nuclear effect obtained for protons of G103, F101, T104, T102, T105, and also for Hδ2 of H99 suggest that corresponding groups are spatially positioned closely to antibody protons of the peptide–antibody complex. Minimal values of transferred nuclear Overhauser effect obtained for protons of A96, E97, and T98 suggest that in

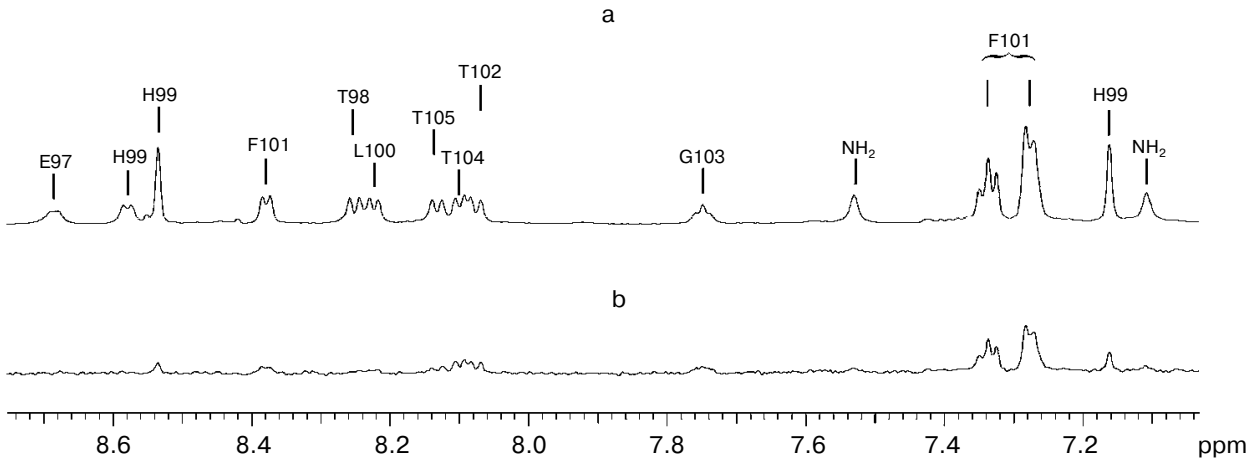

Fig. 5. Region of signals of aromatic and NH protons in the ^{1}H-NMR spectrum of the mixture of monoclonal antibody TA7 and peptide A96-T105 (a) and enlarged (×4) spectrum of nuclear Overhauser effect (b) obtained during application of additional radiofrequency field at 0.5 ppm for 0.6 sec. Concentrations of TA7 and the peptide were 0.17 and 1.3 mM, respectively (pH 5.1, 30°C). Vertical bars show positions of individual amino acid residues on the spectrum.

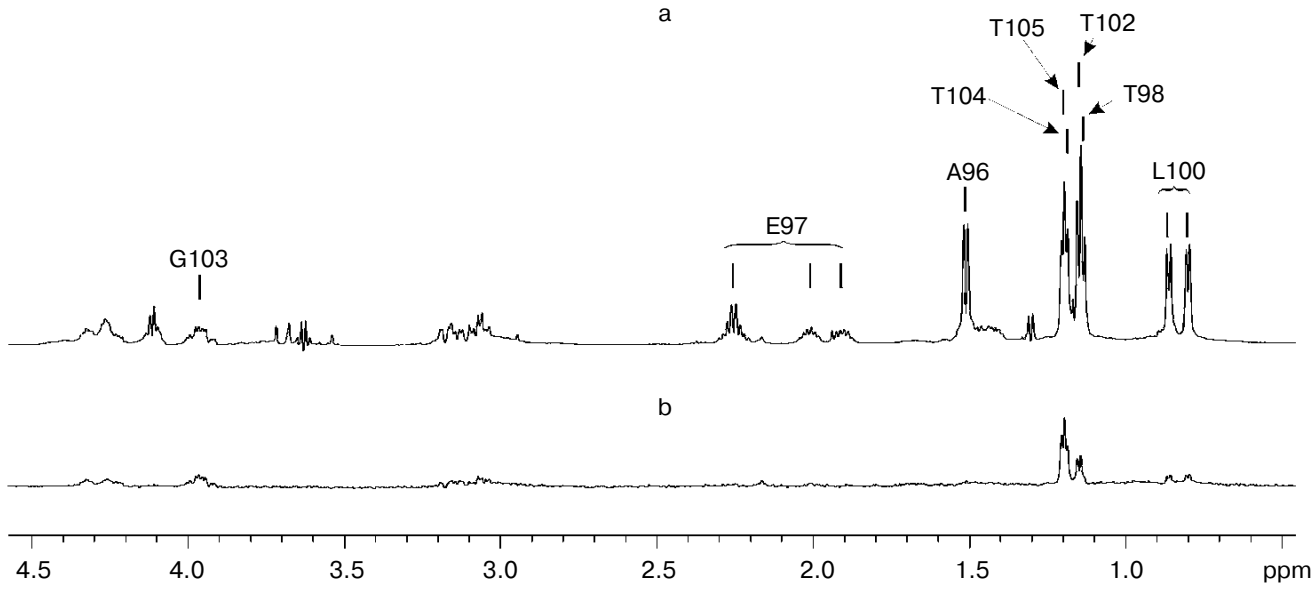

Fig. 6. Region of signals of aliphatic protons in the ^{1}H-NMR spectrum of the mixture of monoclonal antibody TA7 and peptide A96-T105 (a) and enlarged (×4) spectrum of nuclear Overhauser effect (b) obtained during application of additional radiofrequency field at 6.7 ppm for 0.6 sec. Concentrations of TA7 and the peptide were 0.17 and 1.3 mM, respectively (pH 5.1, 30°C). Vertical bars show positions of individual amino acid residues in the spectrum.

the peptide–antibody complex these residues are moved away the antibody surface. Thus, in the peptide–antibody complex the antigen-binding cavity of the antibody accommodates the stretch F101-T105 of the antigen polypeptide chain, whereas the site of antigen polypeptide chain A96-T98 is not involved in binding to antibody and it remains exposed to the solvent. Values of transferred nuclear effect determined for methyl groups of L100 and protons of H99 side chain are characterized by an intermediate mean between maximal (typical for fragment F101-T105) and minimal (typical for fragment A96-T98) values. This suggests that residues H99 and L100 are positioned at the interface of the contact between antigen and antibody surfaces.

The nuclear Overhauser effect appeared in the ligand–macromolecule complex during ligand exchange between free and macromolecule-bound states can be registered on signals of free ligand. This method is widely used for determination of ligand conformation in the ligand–macromolecule complex [24, 25].

Table 2. Transferred nuclear Overhauser effect observed in the peptide–TA7 mixture (8 : 1) (at pH 5.1, 30°C) on signals from protons of the free peptide during application of additional radiofrequency field to signals from antibody protons for 0.2, 0.4, and 0.6 sec (error of the values of transferred effect did not exceed ±1%)

Signal from protons	Transferred nuclear Overhauser effect, %		
	0.2 sec	0.4 sec	0.6 sec
Hα2 G103	5.7	10.0	14.9
Hα1 G103	6.4	9.7	14.5
Hε1, ε2 F101	3.4	7.0	13.1
(Hγ2)3 T104QG	4.1	8.6	12.5
Hδ1, δ2, ζ F101	2.4	6.9	12.3
HN T102	6.0	8.4	11.7
HN T104	3.9	9.2	11.4
HN G103	5.4	7.4	9.3
(Hγ2)3 T105	3.6	5.8	8.8
Hδ2 H99	2.2	3.2	6.6
NH1 T105-NH2	0.6	2.3	6.2
HN T105	2.9	4.9	6.1
(Hγ2)3 T102	1.7	3.4	4.8
HN F101	3.2	4.3	4.7
NH2 T105-NH2		2.1	4.4
Hε1 H99	1.8	2.2	3.4
(Hδ1)3 L100	1.5	1.8	3.0
(Hδ2)3 L100	1.1	1.5	2.9

Note: In ^{1}H-NMR spectrum signals from aromatic protons of F101 represent two multiplets, Hε1,ε2 and Hδ1,δ2,ζ, possessing chemical shifts of 7.35 and 7.31 ppm, respectively.

The presence of cross-peaks between protons CαH of *i*-th and NH of (*i* + 1)-th amino acid residues is a characteristic feature of NOESY spectra of the A96-T105 mixture with monoclonal antibody TA7. It should be noted that with exception of T102 and G103 cross-peaks between NH of *i*-th and (*i* + 1)-th residues were not observed in the NOESY spectrum. Since type one cross-peaks are typical for extended sites of polypeptide chain and type two cross-peaks are characteristic for turns and helical sites our data suggest that the polypeptide chain of the epitope (residues L100-T105) has the extended conformation with a turn around the region of T102 and G103.

The conformation of A96-T105 in the complex with monoclonal antibody was calculated on the basis of volumes of cross-peaks measured in the NOESY spectrum of the mixture A96-T105 with monoclonal antibody TA7. (Time of mixing of longitudinal magnetic components (τ_{mix}) was 0.1 sec). Appearance of cross-peaks in this spectrum was due to nuclear effect induced in the complex A96-T105–TA7 and transferred on signals of free peptide during complex dissociation. Contribution of nuclear effect of the free peptide to the intensity of these cross-peaks is negligible because in the NOESY spectrum of free peptide A96-T105 obtained under similar conditions the cross-peaks are almost indistinguishable from baseline noise. Figure 7 shows the number of cross-peaks of nuclear effect observed between protons of a given residue and neighboring residues and number of cross-peaks of nuclear effect which were absent in the NOESY spectrum (however, their possible presence could not be ruled out *a priori*). These data were used for calculation of spatial structure of A96-T105 in the complex with monoclonal antibody TA7 (see "Materials and Methods" section).

Analysis of square deviation of heavy atom coordinates of the main chain for the resultant set of spatial structures revealed that these deviations are minimal for the site L100-T104 (0.5-1.0 Å) (Fig. 7). Apart from this site the square deviations of heavy atom coordinates sharply increased (in linear dependence on the distance from this site). The increase in square deviations for atom coordinates of T105 may stem from smaller number of experimental limitations for this residue (Fig. 7). Increase of square deviation for atoms at the site A96-H99 suggests that in the peptide–TA7 complex H99 is positioned at the interface of the contact with the antibody surface, whereas residues A96-T98 do not contact the antibody surface and they exhibit conformational flexibility in the antigen–antibody complex. Thus, results of NMR spectroscopy study of the interaction between the synthetic fragment of MLA and monoclonal antibody TA7 indicate that TA7 epitope is formed by the stretch H99-LFTGT-T105 possessing conformation shown in Fig. 8.

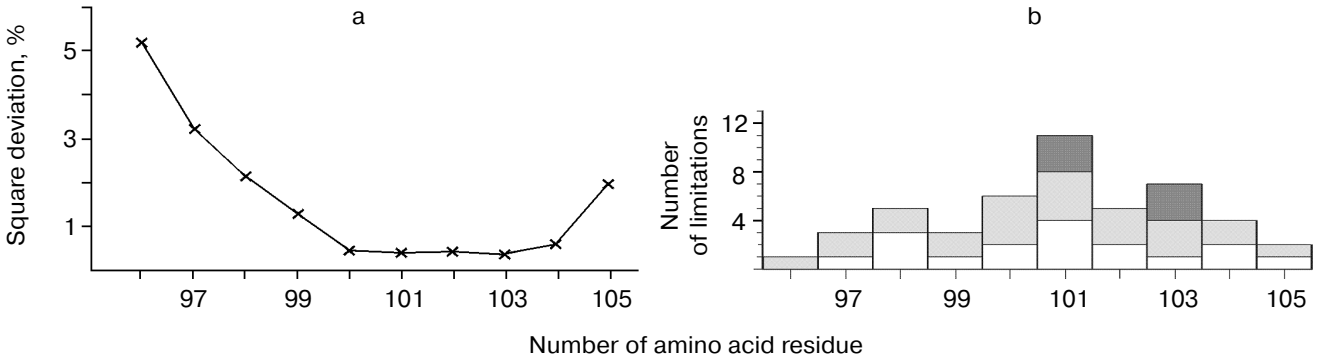

Fig. 7. a) Square deviations of heavy atom coordinates of the main chain for 20 conformers of A96-T105 generated by DYANA software on the basis of experimentally determined limitations on permissible inter-proton distances among peptide protons in the complex with the antibody. b) Experimentally determined upper limitations for permissible inter-proton distances of A96-T105 peptide in the complex with TA7 antibody. Light columns show intra-residue limitations, light-gray columns show limitations between protons of neighboring residues of the polypeptide chain, dark-gray columns show limitations between protons of distant residues of the polypeptide chain.

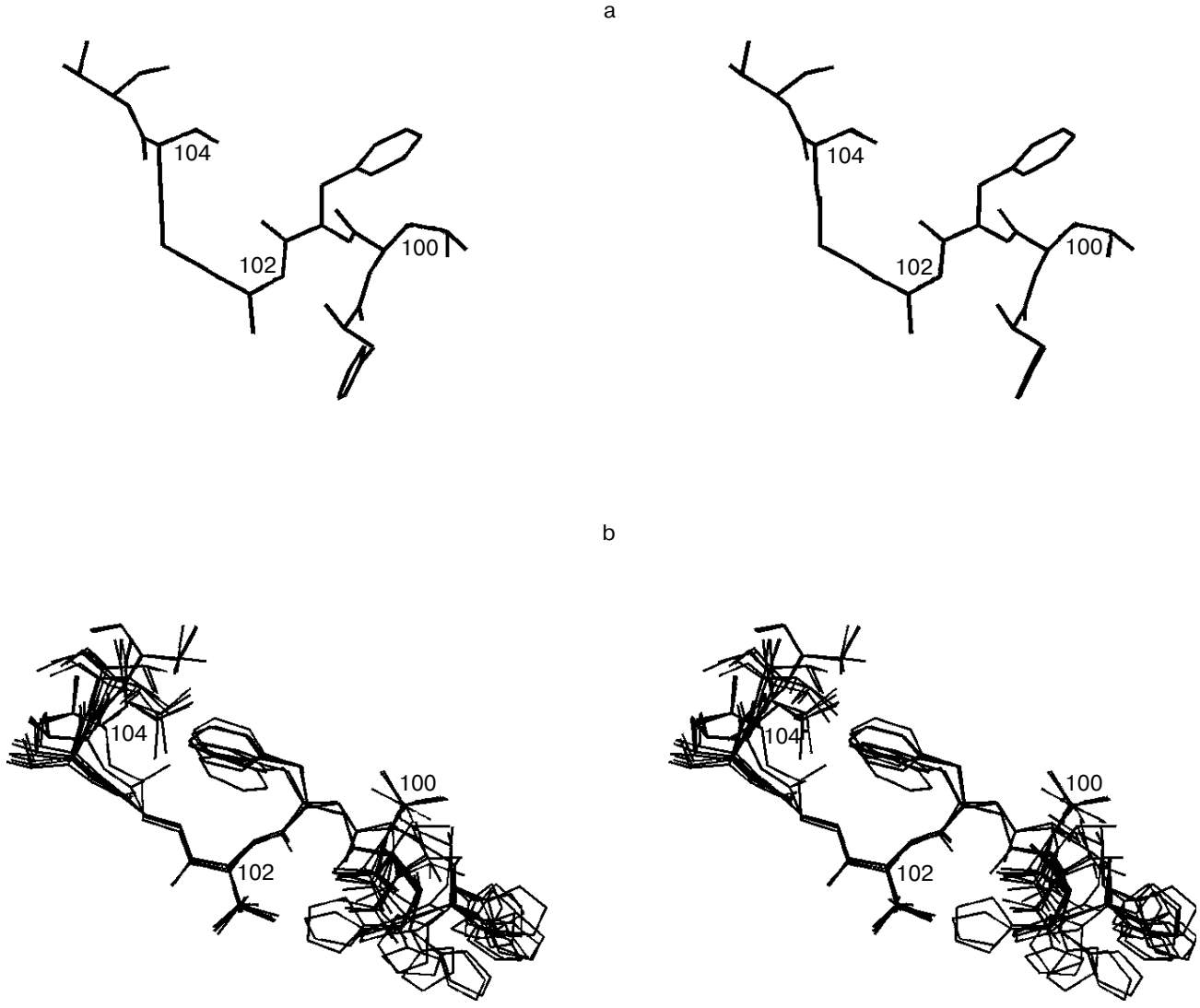

Fig. 8. Spatial structure of the fragment of MLA polypeptide chain H99-T105: a) X-ray model of viscumin H99-T105; b) 20 spatial structures obtained by NMR for the peptide A96-T105–antibody TA7 complex and overlapped by atoms of F101-G103 of the main chain. (Only heavy atoms C, N, and O are shown.)

DISCUSSION

Hybridoma cells represent a unique model for studies of intracellular transport of proteins. Interaction of toxin molecules with antibody inside cellular vesicles complicates transmembrane transfer and inhibition of cytotoxic effect of MLA (Fig. 1). Resistance of TA7 hybridoma cells to viscumin stems from production of the monoclonal antibody TA7 which binds the catalytic subunit of viscumin. The epitope interacting with TA7 is absent in the native protein. The appearance of this epitope occurs after heat denaturation of the toxin or its adsorption on the surface of the immunological plate. Results of the present study provide obtain information about conformational rearrangements of MLA inside vesicles of the target cell.

Comparison of our results with the X-ray model of the viscumin molecule [13] explains why the monoclonal antibody TA7 does not interact with native MLA. In native MLA the fragment L100-T104 forms a loop connecting an α-helix and a bundle of β-sheet. In the complex with TA7 the polypeptide chain has more extended (unfolded) conformation (Fig. 8) and so the aromatic ring of F101, methyl groups of T104 and L100, Cδ2H of H99 and other groups (Table 3) of the antigenic fragment which contact the surface of TA7 within the peptide–antibody complex are hidden by protein globule in native MLA.

During protein adsorption on the immunological plate resulting in partial unfolding of MLA two groups of antibodies have been recognized. Hybridoma cells synthesizing monoclonal antibodies against the denatured form of viscumin (and constituting the second group of antibodies such as monoclonal antibody TA71) were not resistant to the toxin. These antibodies did not recognize their particular epitope inside cells. This may be explained by the absence of intracellular changes in toxin conformation favoring exposure of the given epitope. It is also possible that the toxin–antibody complex is not formed due to epitope shielding by other proteins and/or membrane.

Our data suggest that inside cellular vesicles (and, consequently, during intracellular transport) MLA under-

Table 3. Comparison of X-ray data on susceptibility of individual hydrogen atoms of the fragment H99-T105 of catalytic A-subunit of viscumin to solvent (1.4 Å) with NMR data on relative contact of peptide groups with the surface of TA7 in the peptide–antibody complex

Amino acid residue	Relative susceptibility, %		
	hydrogen atoms	X-ray analysis*	^{1}H-NMR**
H99	HN	0.0	<15
H99	Hδ2	0.0	44.3
H99	Hε1	72.0	22.6
L100	HN	0.0	<15
L100	Hδ11, δ12, δ13	0.0, 13.4, 7.5	19.3
L100	Hδ21, δ22, δ23	0.0, 0.0, 5.4	20.4
F101	HN	66.7	31.6
F101	Hδ1, δ2, ζ	0.0, 71.9, 0.0	82.6
F101	Hε1, ε2	0.0, 2.2	88.0
T102	HN	83.3	78.6
T102	Hγ21, γ22, γ23	100.0, 85.5, 97.4	32.1
G103	HN	83.3	62.7
G103	Hα1	51.2	97.5
G103	Hα2	100.0	100.0

* Susceptibility of hydrogen atoms to the solvent in the isolated amino acid residue was denoted as 100%.

** Data were calculated from the ratio of values of transferred nuclear Overhauser effect observed on signals of free peptide in the mixture of peptide and TA7 (τ_{ir} = 0.6 sec); relative susceptibility of Hα2 G103 to the antibody surface was denoted as 100%.

goes structural changes. This is consistent with data for another plant toxin, ricin, which shares some structural similarity with viscumin. Introduction of a covalent disulfide bond into the A-subunit of ricin prevented protein unfolding and reduced toxin ability for translocation through the vesicular membrane; this reduced cytotoxic activity of ricin [26]. In the case of A-subunit of ricin it was demonstrated that formation of so-called "molten globule" state preceded protein translocation across the membrane of intracellular vesicles [27]. This state is characterized by partial protein unfolding followed by subsequent restoration of its native structure in the presence of eukaryotic ribosomes *in vitro*.

Factors influencing the structure of the toxin catalytic subunit inside cellular vesicles remain unknown. It is possible that structural change may results from A-subunit interaction with membrane and/or protein carriers.

The authors are grateful to E. F. Kolesanova for her help in peptide synthesis on polyethylene needles. We also thank A. S. Arseniev for useful discussion of data obtained and his help in preparation of this paper.

This work was partially supported within the framework of an agreement between the Ministry of Science and Technology of Russian Federation and the Ministry of Education and Scientific Studies of Germany (project RUS 01/237).

REFERENCES

1. Barbieri, L., Battelli, M. G., and Stirpe, F. (1993) *Biochim. Biophys. Acta*, **1154**, 237-282.
2. Saavedra-Lozano, J., McCoig, C., Xu, J., Cao, Y., Keiser, P., Ghetie, V., Siliciano, R. F., Siliciano, J. D., Picker, L. J., Ramilo, O., and Vitetta, E. S. (2002) *J. Infect. Dis.*, **185**, 306-314.
3. Day, P. J., Owens, S. R., Wesche, J., Olsnes, S., Roberts, L. M., and Lord, J. M. (2001) *J. Biol. Chem.*, **276**, 7202-7208.
4. Kende, M., Yan, C., Hewetson, J., Frick, M. A., Rill, W. L., and Tammariello, R. (2002) *Vaccine*, **20**, 1681-1691.
5. Deeks, E. D., Cook, J. P., Day, P. J., Smith, D. C., Roberts, L. M., and Lord, J. M. (2002) *Biochemistry*, **41**, 3405-3413.
6. Agapov, I. I., Tonevitsky, A. G., Moysenovich, M. M., Maluchenko, N. V., Weyhenmeyer, R., and Kirpichnikov, M. P. (1999) *FEBS Lett.*, **452**, 211-214.
7. Lord, J. M., Davey, J., Frigerio, L., and Roberts, L. M. (2000) *Semin. Cell Dev. Biol.*, **11**, 159-164.
8. Agapov, I. I., Tonevitsky, A. G., Maluchenko, N. V., Moisenovich, M. M., Bulah, Y. S., and Kirpichnikov, M. P. (1999) *FEBS Lett.*, **464**, 63-66.
9. Tonevitsky, A. G., Shamshiev, A. T., Prokoph'ev, S. A., Agapov, I. I., and Toptygin, A. Yu. (1995) *Immunol. Lett.*, **46**, 5-8.
10. Kornfeld, S. B., Leonard, J. E., Mullen, M. D., and Taetle, R. (1991) *Cancer Res.*, **51**, 1689-1693.
11. Tonevitsky, A. G., Zhukova, O. S., Mirimanova, N. V., Omelyanenko, V. G., Timofeeva, N. V., and Bergelson, L. D. (1990) *FEBS Lett.*, **264**, 249-252.
12. Tonevitsky, A. G., Marx, U., Agapov, I., and Moisenovich, M. (2002) *Arzneimittelforschung*, **52**, 67-71.
13. Sweeney, E. C., Tonevitsky, A. G., Palmer, R. A., Niwa, H., Pfueller, U., Eck, J., Lentzen, H., Agapov, I. I., and Kirpichnikov, M. P. (1998) *FEBS Lett.*, **431**, 367-370.
14. Kabsch, W., and Sander, C. (1983) *Biopolymers*, **22**, 2577-2637.
15. Jameson, B. A., and Wolf, H. (1988) *Comput. Appl. Biosci.*, **4**, 181-186.
16. Kolesanova, E. F., Kozin, S. A., Rumyantsev, A. B., Jung, C., Hoa, G. H., and Archakov, A. I. (1997) *Arch. Biochem. Biophys.*, **341**, 229-237.
17. Mossman, T. (1983) *J. Immunol. Meth.*, **65**, 55-63.
18. Piotto, M., Saudek, V., and Sklenar, V. (1992) *J. Biomol. NMR*, **2**, 661-665.
19. Balashova, T. A., Pashkov, V. S., Onoprienko, L. V., Mikhaleva, I. I., Mareeva, T. Yu., Petrova, E. E., Nesmeyanov, V. A., and Ivanov, V. T. (1991) *Bioorg. Khim.*, **17**, 1470-1486.
20. Guntert, P., Mumenthaler, C., and Wuthrich, K. (1997) *J. Mol. Biol.*, **273**, 283-298.
21. Koradi, R., Billeter, M., and Wuthrich, K. (1996) *J. Mol. Graph.*, **14**, 51-55.
22. Carayon, P., Bord, A., Gaillard, J. P., Vidal, H., Gros, P., and Jansen, F. K. (1993) *Bioconjug. Chem.*, **4**, 146-152.
23. Hopp, T. P., and Woods, K. R. (1983) *Mol. Immunol.*, **20**, 483-489.
24. Roberts, G. C. K. V. (1999) *Curr. Opin. Struct. Biol.*, **10**, 42-47.
25. Ni, F. (1994) *Progress in NMR Spectroscopy*, Vol. 26 (Emsley, J. W., Feeney, J., and Sutcliffe, L. H., eds.) Pergamon Press, Oxford-New York-Toronto-Sydney-Frankfurt, pp. 517-606.
26. Beaumelle, B., Taupiac, M. P., Lord, J. M., and Roberts, L. M. (1997) *J. Biol. Chem.*, **272**, 22097-22102.
27. Argent, R. H., Parrott, A. M., Day, P. J., Roberts, L. M., Stockley, P. G., Lord, J. M., and Radford, S. E. (2000) *J. Biol. Chem.*, **275**, 9263-9269.